Phase Transition and Domain Morphology of Siloxane-Containing Hard-Segmented Polyurethane Copolymers

W. C. Tsen, F. S. Chuang

Department of Polymer Materials, Vanung University, Tao-Yuan, Taiwan 32045, Republic of China

Received 30 March 2005; accepted 1 September 2005
DOI 10.1002/app.23087
Published online in Wiley InterScience (www.interscience.wiley.com).

ABSTRACT: The phase transitions and the morphology of hard-segment domains of those siloxane-containing hard-segmented polyurethane copolymers are studied by differential scanning calorimetry (DSC). The NH-SiPU2 copolymer, which comprises a siloxane–urea hard segment and a polytetramethylene ether glycol soft segment (PTMG2000), exhibits a high degree of phase-separation and a highly amorphous structure. Therefore, NH-SiPU2 copolymer proceeds with a melt-quenching process and with various annealing conditions, to examine the morphologies and the endothermic behaviors of the siloxane-containing hard-segment domains. DSC thermograms of further annealed NH-SiPU2 indicate that the first endotherm (T_1) at around 75°C is related to the short-range ordering of amorphous siloxane hard-segment domains (Region I), and the second endotherm (T_2) at around 160°C is related to the long-range ordering of amorphous siloxane hard-segment domains (Region II). The DSC thermograms at annealing temperatures below and above T_1 demonstrate that both the temperature and the enthalpy of T_1 linearly increase with the logarithmic annealing time (log t_a). This result shows that the endothermic behavior of T_1 is typical of enthalpy relaxation, which is caused by the physical aging of the amorphous siloxane hard segment. Additionally, the siloxane hard segments in Region I are movable, and can merge with the more stable Region II under suitable annealing conditions. Transmission electron microscopy shows that Regions I and II are around 200 and 800 nm wide, and that the Region I can be combined with the stable Region II, under suitable annealing conditions. © 2006 Wiley Periodicals, Inc. J Appl Polym Sci 101: 4242–4252, 2006

Key words: siloxane; polyurethane; endothermic behavior; morphology; domain

INTRODUCTION

Segmented polyurethanes (PUs), which comprise hard and soft segments, are widely used in thermal plastic elastomers, owing to their excellent mechanical and chemical characteristics. However, the mechanical stability of PUs are low at high temperatures,[1,2] and their initial temperature of degradation is typically around 200°C, which is near their melting temperature.[2–5] Therefore, the mechanical characteristics and thermal stability are improved by altering the structure of the segments, such as by incorporating into the hard or the soft segment an aromatic amide,[6] an aromatic imide,[3] or a silicone group.[4,5] The degradation and stability of various PUs have been studied by thermogravimetric analysis (TGA),[2–8] subambient thermal volatilization analysis,[9] mass analysis based on direct pyrolysis, and TG combined with other techniques (TG-mass or TG-GC).[10,11] The studies demonstrate that the first step of the degradation of PUs is governed by a hard segment that normally comprises a pure urethane group or a urea group. The second step in the degradation originates in the soft segment, which is usually an ester-type or an ether-type polyol. Although the hard and soft segments of PUs influence the stability of thermal degradation, the morphology of the domains that consist of hard segments also, importantly, affects the mechanical stability in practical application.

Differential scanning calorimetry (DSC) has been employed to analyze the morphology of PU domains. Several references[12,13] have suggested that the DSC thermograms of PUs appear at least four phase-transition temperatures; they thus have two melting points (if both phases crystallize) and two glass transition temperatures, since they have a two-phase structure.[12] Hesketh et al.[13] found that the glass transition temperature (T_g) of the soft-segment domains on ester or ester-type PU was between −80 and −10 °C, depending strongly on the length of the molecular chain and the degree of phase-separation. The melting endotherm of the soft segment (T_ms) was between 10 and 20°C, when the soft segment contained sufficiently long molecular chains.[2,12,13] The DSC thermogram of the hard-segment domains typically exhibits multiple and broad endotherm peaks, because the thermal history (annealing effect) causes the hard-

Correspondence to: W. C. Tsen (charity@msa.vdu.edu.tw).
Contract grant sponsor: National Science Council, Republic of China; contract grant number: NSC 91–2622-E-238–003.

segment domains to form various morphologies. The endothermic behaviors of the hard-segment domains, which include multi-endothermic regions at around 80 or 160°C, were uncertain, or may have various causes, such as the destruction of urethane hydrogen bonds[14,15] or the morphology of the short-range and long-range ordered hard-segment domain.[16] The microcrystallization of the hard segment, which was verified to occur at over 200°C, was evident in materials with a long aromatic urethane segment[17] or a high hard-segment content.[2] Infrared spectroscopy indicated that hydrogen bonds remained important at 200°C, and DSC analysis demonstrated that the ΔH and ΔS values varied slowly, contributing only a little to the observable thermal response.[16] Therefore, the DSC multi-endotherm peaks of the hard segments demonstrate that the morphological effect is stronger than the hydrogen bond effect. Many works [16,18,19] have established that the DSC thermogram of PUs includes three endotherms regions, associated with the hard-segment domains. The first endotherm (Region I), observed between 30 and 90°C, was generally attributed to an unknown short-range ordering. The second endotherm (Region II) in the range 120–190°C was associated with the long-range ordering of hard segments in an unspecified fashion, or with the onset of microphase mixing between the hard and soft segments.[18,19] Finally, a large endotherm (Region III), which was present at around 200°C, was attributed to the melting of the microcrystalline hard segment. However, PUs with a low diisocyanate content could not crystallize, and exhibited only Regions I and II.[16,20]

Several works [21–23] have investigated the crystalline morphology of typical urethane hard-segment domains, using DSC, polarization microscopy, transmission electron microscopy (TEM), and other techniques. However, the amorphous morphology of urethane hard-segment domains has seldom been investigated. The morphology and the domain structures of siloxane-containing hard segments have not yet been considered. Therefore, this work focuses on the morphology of two phases and the endothermic behavior of the morphology. It investigates the morphology and the domains of siloxane-containing hard segmented PU, using DSC and TEM technology.

EXPERIMENTAL

Materials

The authors[5] reported elsewhere the synthesis and structures of siloxane-containing PU copolymers, whose compositions are presented in Table I. The copolymer's hard segment comprises various siloxane chain-extenders, such as 4,4′-diphenylmethane diisocyanate (MDI), and the soft segment consists of polytetramethylene ether glycol (M_w = 2000, PTMG 2000; or M_w = 1000, PTMG1000, respectively), as shown in Figure 1.

TABLE I
Hard-Segment Content

Sample	Si-urethane-HSC[a] (wt %)	Si-urea-HSC[b] (wt %)	Hard-segment number-average molecular weight ($M_{w\,nh}$)[c]
OH-SiPU1	43.8	—	779
OH-SiPU2	28.0	—	778
NH-SiPU1	—	42.8	748
NH-SiPU2	—	27.2	747

[a] Siloxane-containing urethane hard segment content.
[b] Siloxane-containing urea hard segment content.
[c] The hard segment number-average weight was calculated by method[8] of $M_{w\,nh}=M_{ns}(100 - S_c/S_c)$ where $M_{w\,nh}$ is the hard segment number-average weight, M_{ns} is the soft segment number-average weight, and S_c is the soft segment content (wt %).

Differential scanning calorimetry

The DSC measurement was made using a Perkin–Elmer Pyris 1 DSC with ice water and liquid nitrogen cooler. Indium was used to calibrate the temperature and heat of fusion. The mass of the specimens was roughly 5 mg. The initially scanned specimens were the untreated samples, which had been stored in a desiccator below 30°C, for 7 days, before any DSC analysis. The initial scan of those specimens proceeded from −100 to 230°C at the rate of 20°C/min in an atmosphere of nitrogen. The melt-quenched specimens (second scan) were the same as those in the initial scan. First, the specimens were heated to 230°C and held at this temperature for 1 min, to eliminate their thermal history. They were then quenched to −110°C at a rate of 300°C/min. Subsequently, the thermograms of the specimens were obtained at a heating rate of 20°C/min from −100 to 230°C.

The annealed samples were prepared as for the second scan. They were first heated to 230°C and held at this temperature for 1 min, to eliminate their thermal history; they were then quenched to 20°C at a rate of 300°C/min, at which temperature they were maintained until thermal equilibrium was reached. Thereafter, the thermograms of the samples were obtained at a heating rate of 20°C/min. The mass of each sample was ~5 mg. The endothermic temperatures of the hard segment domains (Regions I and II) exceeded room temperature herein, and so the DSC thermograms of the melt-quenched samples were measured only above room temperature, under various annealing conditions. Figures 5, 7, 8, and 10–12 presented the various annealing conditions. Additionally, a test tube full of nitrogen was used in the samples that underwent annealing for over 24 h. Then, the test tube was

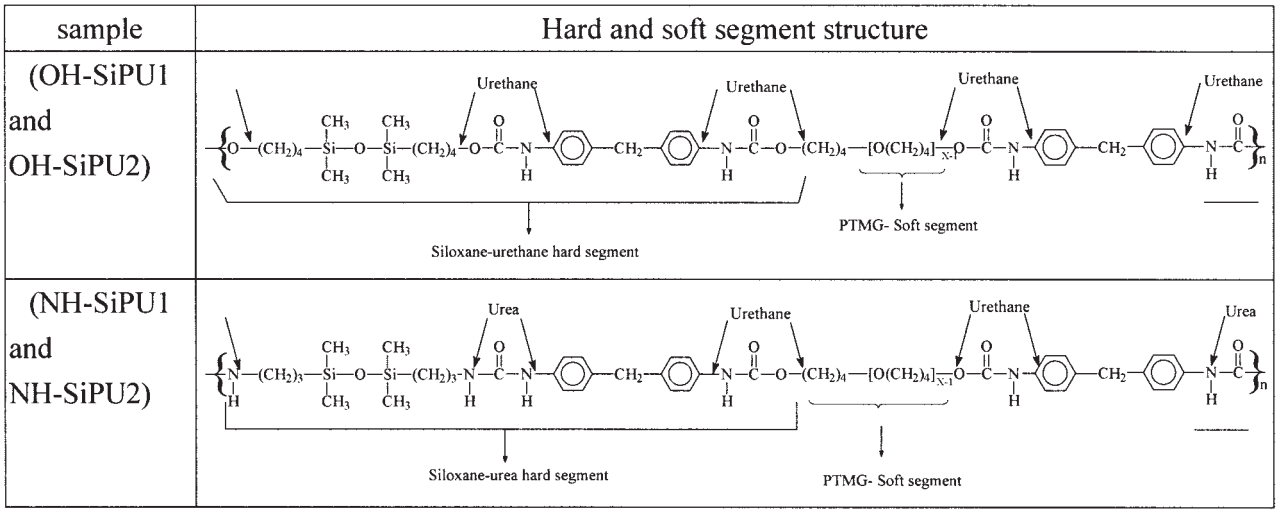

Figure 1 Structure of siloxane-containing segmented PU copolymers.

placed in a vacuum oven and maintained at a constant temperature for a predescribed period.

The magnitude of the enthalpy relaxation, caused by annealing, was calculated from the net area obtained, by subtracting the DSC thermogram of an unaged sample from that of an aged one. This method is the generally accepted technique, according to the literature.[24,25]. The peak position was measured by using vertical cursors to locate the peak position.

Transmission electron microscopy

TEM was performed using a JEOL JEM 200CX instrument operated at 100 kV. The melt-quenched specimens, after annealing under various conditions, were enclosed in epoxy resin and cut into ultrathin sections. Then, the microtomed specimens were stained with RuO_4 and examined on copper grids (300 mesh), without any supporting film.

Wide-angle X-ray diffraction

Wide-angle X-ray scattering experiments were conducted on the samples, using a Diano 8536 X-ray diffractometer. The X-ray beam was a nickel-filtered Cu Kα radiation (λ = 0.1542 nm) from a sealed tube, operated at a voltage of 30 kV and a current of 30 mA. Data were obtained while scanning at a rate of 4°/min from 5 to 60°.

RESULTS AND DISCUSSION

Phase transition regions

The morphology of the segmented PU copolymers has a two-phase microstructure, because the two dissimilar segment types are incompatible. Therefore, DSC thermograms of PUs probably exhibit four transition regions, if both phases crystallize. However, the structure and concentration of the hard and soft segments, the molecular weight of the soft segments, the degree of phase separation, and the thermal history influenced the endotherms of the phase transition regions in the DSC thermograms [13,26,27]. Therefore, they determined whether the phase transition regions were unclear or invisible in the DSC thermograms. Figure 2 presents the initial scanning DSC thermograms of the untreated samples, including three or four phase transition regions.

Soft-segment transition region

The untreated samples in the first transition region of the DSC thermograms exhibited a baseline shift from −80 to −10°C, as shown in Figure 2. This region is

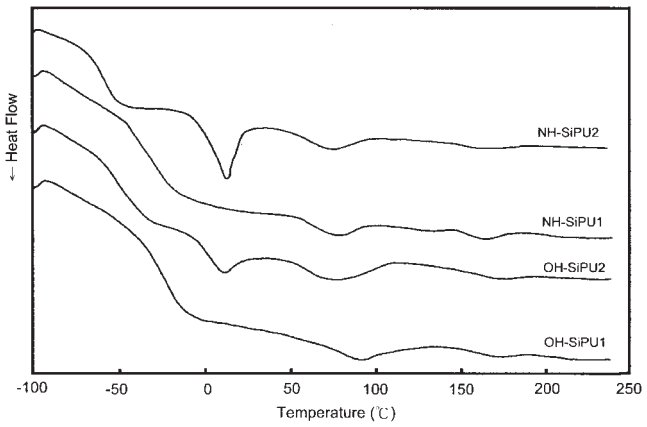

Figure 2 DSC thermograms of the initial scan for all untreated samples.

TABLE II
Phase Transition Temperatures

	Initial scan				Melt-quenching scan			
Sample	T_g[a] (°C)	T_m[b] (ΔH kJ/mol)	T_1[c] (°C)	T_2[c] (°C)	T_g[a] (°C)	T_m[b] (ΔH kJ/mol)	T_1[c] (°C)	T_2[c] (°C)
NH-SiPU2	−69	15(41)	71	—	−67	7(9)	75	—
NH-SiPU1	−47	–	79	165	−40	–	83	160
OH-SiPU2	−58	13(25)	77	–	−51	–	80	–
OH-SiPU1	−38	–	89	–	−23	–	–	–

[a] The soft-segment glass temperature determined by the intersection of the baseline and a tangent through midpoint.
[b] The soft-segment melting temperature is the peak value.
[c] T_1 and T_2 are the temperatures of endothermic peaks and are related to the amorphous siloxane hard-segment.

considered to be associated with a soft-segment glass transition temperature (T_g) that is typically affected by the hard-segment content, the molecular weight of the segments, and the affinity of one segment for other. The T_g value indicates the relative purity of the soft-segment regions, and so it is related to the degree of phase-separation.[13]

Table II reveals that the T_g values of the untreated samples (OH-SiPU1 and NH-SiPU1) in the initial scan appeared at around −38 and −47°C. The T_g of NH-SiPU1 is lower than that of OH-SiPU1, for the same soft-segment length and a near-hard-segment content, because NH-SiPU1 has strong intermolecular hydrogen bonds among the siloxane urea groups of the hard segments, which restrict the movement of the hard segments into soft-segment regions. Fewer soft-segment domains of NH-SiPU1 are contaminated with hard segments, and so the sample has purer soft-segment phases. That is, the two-phase structure of NH-SiPU1 exhibits less mixing between hard and soft segments (a high degree of phase-separation). Similar results were obtained for the OH-SiPU2 and NH-SiPU2 samples, when the soft segment had the PTMG 2000 composition, as indicated by Table II. Additionally, the length of the soft segment strongly affects the glass transition temperature. In this work, the samples (OH-SiPU2 and NH-SiPU2) with a long soft segment had lower T_g values than the samples with short soft segments (OH-SiPU1 and NH-SiPU1), as shown in Table II. This result also indicates that the longer segment of the former has less compatibility.[13] The earlier results indicate that the hard-segment type and soft-segment length affect the T_g and the phase-separation of the copolymers. The NH-SiPU2 sample in this work, which exhibits greater phase-separation than the other samples, because of the greater incompatibility of its hard and soft segments, has the lowest T_g.

As the temperature of the DSC curves exceeded to 0°C, as shown in Figure 2, a large endotherm peak, which was associated with the crystalline morphology of the soft-segment, appeared at 15°C (the melting temperature of soft-segment: T_m). It was obtained only from the samples (OH-SiPU2 and NH-SiPU2) with the long soft segments. The OH-SiPU1 and NH-SiPU1 exhibited no soft segments of melting endotherm, because both had short soft segments (PTMG1000), which were responsible for strong steric restriction.[2]

Hard-segment transition region

The DSC thermograms from the initial scan of the untreated samples exhibited two broad endotherms at 50–110°C(T_1) and 150–190°C(T_2), outside the soft-segment transition region, as presented in Figure 2. The temperature regions of the first and second endotherm (T_1 and T_2) are the hard segment transition regions in which morphology is, respectively, the short-range and long-range ordering of the hard-segment domains (Regions I and II) [13,16,26–28].

The T_1 of the NH-SiPU2 and NH-SiPU1 samples between 50 and 100°C were narrower than those of the OH-SiPU2 and OH-SiPU1 samples, whose T_1 regions covered the range of 50–120°C. NH-SiPU2 and NH-SiPU1 have a narrow T_1, which reflects higher phase-separation or more well-defined hard-segment domains.[4,27] This result also shows that the siloxane–urea hard segments were more likely to have formed a Region I than did the siloxane–urethane hard segments, because the siloxane–urea hard segments had very strong intermolecular hydrogen bonds.

The second endotherm (T_2) for the other samples except NH-SiPU1, did not show a distinct endothermic peak, as presented in Figure 2, because the hard segments are short, as the samples consisted of two hard-segment units (including two MDI units and one chain-extender unit; M_{nh} = 750). Therefore, long hard segment domains cannot easily be aggregated under the preparation conditions used in this work. However, the NH-SiPU1 sample with a high content of siloxane–urea hard-segment has a clear endotherm in Region II, because such hard segments have numerous hydrogen bonds. The result reveals that the urea hard-segments easily aggregate into long-range ordered domains. Appropriate annealing conditions can also promote the formation of the Region II structure, except for the effect of the strong hydrogen bond, because the

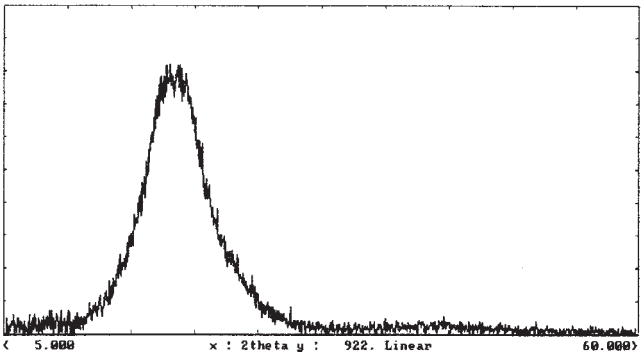

Figure 3 WAXD intensity of the untreated NH-SiPU2 sample.

hard segments with short-range order can merge with the hard segment domains with long-range order.[27] This phenomenon is discussed in the following sections (under Results and Discussion), and is confirmed by the effect of annealing and by TEM.

Many studies[13,16,26,27] have reported that three hard-segment transition regions appear on the DSC thermograms of the untreated samples. They suggest that both Regions I and II were amorphous hard-segment domains, and the third region of the hard-segment domain (Region III) exhibited crystallization. However, a sample with a lower hard-segment content cannot form crystals, because it did not have sufficiently long hard-segment domains. The literature[28] suggests that PUs hard segments with over three MDI units and could generate stable crystals. The 2θ wide-angle X-ray diffraction (WAXD) scan of the crystalline hard-segment domains of the PUs yielded several sharp peaks at 15–28°, with a Bragg spacing between 4.9 and 3.51 Å.[28] Figure 3 shows that the WAXD intensity of the untreated sample (NH-SiPU2) was a highly amorphous structure, indicating that the endothermic peaks of T_1 and T_2 are the second transition that is related to the amorphous siloxane hard segments. The amorphous sample can be used to study the amorphous morphology of the hard segments. Other samples yield WAXD results that are similar to those obtained for the NH-SiPU2 sample, which has the highest phase-separation over any in this work.

Phase transition regions under melt-quenching

The DSC thermograms (Fig. 2) have a clear thermal history, because all samples were heated at 80°C for 8 h to remove the DMF solvent before they were dried by vacuuming at 60°C and stored in a desiccator at 25°C for 7 days before the initial DSC scan. Melt-quenching effectively eliminates thermal history, and so the flowing sections of the melt-quenched and annealed samples were used to elucidate the morphologies of various transition regions of the hard-segment phase, as well as the endothermic behaviors.

Soft-segment phase

Figure 4 presents DSC thermograms of the melt-quenched scan. The temperature of the soft segment transition (T_gs) of the melt-quenched samples shifts upward, as presented in Table II. This result reveals that heating promotes phase mixing and reduces the purity of the soft domains. However, the T_g value of NH-SiPU2 is almost unchanged at around −69°C, following melt-quenching. This result shows that barely any phase mixing occurred in NH-SiPU2. Therefore, NH-SiPU2 exhibits greater phase-separation than the other samples herein.

Only NH-SiPU2 exhibited the melting temperature of the soft segment (T_m) after melt-quenching. Additionally, the T_m value shifted back toward a lower temperature and the enthalpy of the endotherm declined, as shown in Table II. The result indicates that the degree of phase-separation in NH-SiPU2 is strong, and so the hard-segment domains exerted a weaker filler effect, allowing the soft segment to crystallize. The crystallization at a lower temperature resulted in a lower T_m and enthalpy, yielding smaller crystals and a less-ordered crystalline structure. Melt-quenching changed the state of the other samples from crystalline soft segment to amorphous, because phase mixing was extensive, and mixing the hard segments into soft-segment regions restricted the crystallization of the soft segments.

Hard-segmented phase

The endotherm regions (T_1 and T_2) of the melt-quenched samples were flatter and broader than those of the untreated samples, eventually disappearing from the DSC thermograms, as shown in Figure 4.

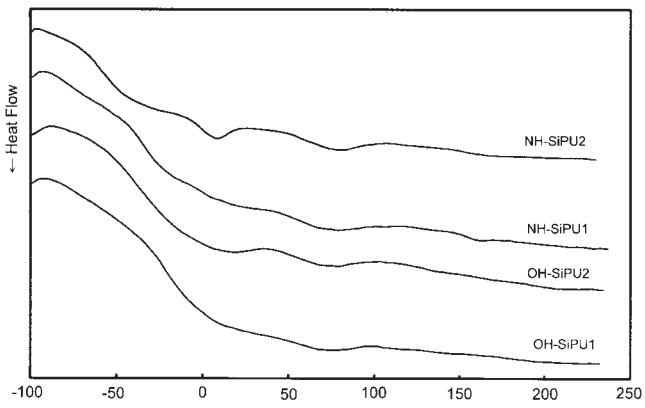

Figure 4 DSC thermograms of the melt-quenched scan for all untreated samples.

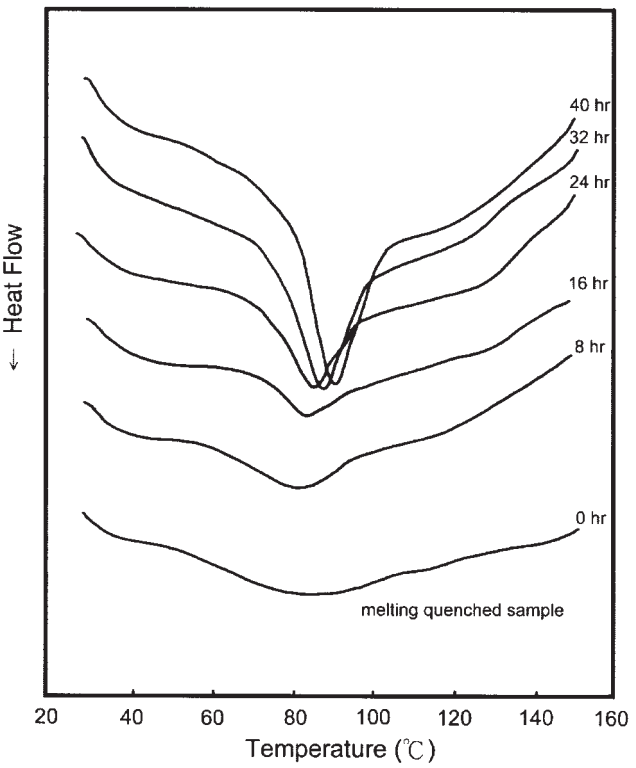

Figure 5 DSC thermograms of the melt-quenched NH-SiPU2 samples, which were annealed at 60°C for different periods.

This diminution or disappearance of endothermic behavior from the melt-quenched scan suggested that quenching was too rapid for ordered structures (Regions I and II). The structures after melt-quenching are therefore difficult to reform again. According to the literature,[29,30] the flat endotherm and the small endothermic peak are attributable to the disorderly Regions I and II or the lower degree of ordering. However, this phenomenon (a reduced or absent endotherm) can be promoted by annealing for a long period.[27,31]

Endothermic behaviors and morphology of hard-segment phases

As mentioned earlier, the hard-segment domains (Regions I and II) of the untreated samples are normally more ordered or have a more complete structure than the melt-quenched samples. In fact, the untreated samples exhibit a thermal history, including an annealing temperature (T_a) and time (t_a), which govern the formation of the domains. Suitable annealing conditions may increase the completeness of the structure of the hard-segment domains, and so this section investigates the relationship between the endothermic behaviors of the hard-segment domains and their morphology, under various annealing conditions.

The endothermic behavior and the effect of annealing on the soft-segment phase have been addressed in the literature,[13] suggesting that the degree of mixing of the two phases and the crystallization clearly affected the changes of T_g and T_m. Furthermore, the soft-segment phase was clearly a melted state above room temperature. The hard-segment phase, which reinforces the soft-segment phase, acts as filler particles dispersed in the soft-segment phase, while hard-segment domains at room temperature strongly influence the physical characteristics of PU copolymers. Hence, the change in the soft segment-phase and the stabilization of the structure by annealing was not considered herein.

The melt-quenched NH-SiPU2 sample exhibited a high degree of phase-separation and amorphous hard-segment phases, and so the sample was annealed under various conditions to elucidate the relationship between the endothermic behaviors and the amorphous morphology of the siloxane hard-segment domains. The following DSC thermograms of the melt-quenched samples were measured only at room temperature, because the endothermic regions (T_1 and T_2) of the siloxane hard-segment domains were generally above room temperature.

Endothermic behavior and morphology of Region I

Figure 5 presents the DSC thermograms of the melt-quenched NH-SiPU2 samples after further annealing at 60°C, for various periods. A small endotherm, which shifted to a higher temperature, appeared near T_1, as shown in Figure 5. Additionally, the enthalpy increased with the annealing time (t_a). Figure 6 plots a linear relationship between the logarithm of annealing time (log t_a) and both the enthalpy (ΔH) of the endo-

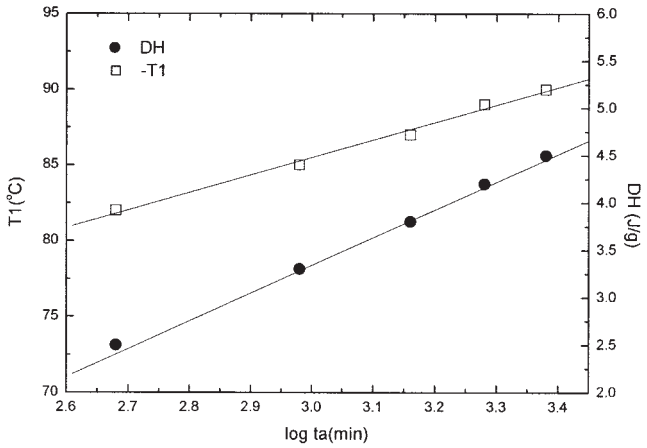

Figure 6 (a) Relationship of the endotherms magnitude, ΔH, and (b) Relationship of the endothermic peak position, T_1, with respect to the logarithm of the annealing time. Both (a) and (b) result from the DSC thermograms in Figure 5.

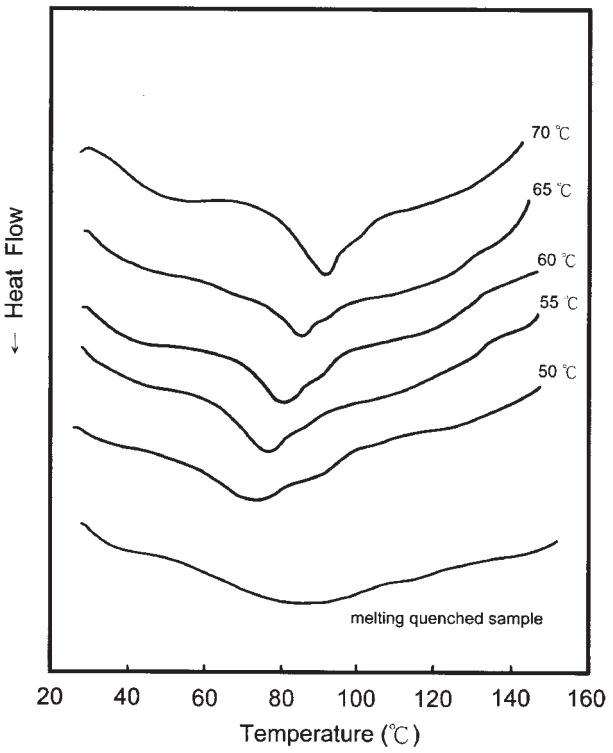

Figure 7 DSC thermograms of the melt-quenched NH-SiPU2 samples, which were further annealed under different annealing temperatures, T_a, for 24 h.

therm and its peak position, T_1. This plot reveals that well-ordered siloxane hard-segment domains (Region I) can be formed more effectively after annealing at 60°C for different periods. Figure 7 displays DSC thermograms of the melt-quenched NH-SiPU2 samples after they had been further annealed at various temperatures (T_a) for 24 h. The highest endothermic peak appeared at $T_a \approx T_1$ (T_g) − 20°C. The results in Figures 5–7 were compared with those obtained by Tenbrinke and Grooten, who[32] reviewed all the enthalpy relaxation behaviors that are related to the physical aging of the amorphous polymers. The results are summarized as follows:

1. The enthalpy of the endothermic peak near T_g increases linearly with the logarithm of the annealing time (t_a), when the aged glass is not in equilibrium.[25,26,33–36]
2. The position of the endothermic peak also increases linearly with log t_a under the same conditions.[24,34,37,38]
3. The maximum height of the endothermic peak is a function of annealing temperature when $T_a = T_g - 20$°C.[34,39]

Therefore, the endothermic behavior of NH-SiPU2 polymer in Region I during sub-T_1 annealing (at a temperature below T_g) may have been an enthalpy relaxation behavior, caused by the physical aging of amorphous silioxane–urea hard segments. The aging behavior was, in fact, caused by the inherent lack of equilibrium of the glass state. During cooling, the molecules could not reach their equilibrium conformation with respect to temperature, because viscosity increased rapidly and the associated molecular mobility declined as T_g approaches. Therefore, the thermodynamic potential existed for the molecules to approach equilibrium by undergoing further packing and conformational change. The molecular mobility below T_g, although greatly reduced, remained finite, enabling the polymer molecules to approach the equilibrium state, as in normal liquid-like packing. The measurable thermodynamic state functions, enthalpy and free volume, have been found to drop as the sub-T_g annealing time increased, for amorphous glassy polymers.[32]

Cooper and coworkers[13,29] posited that the low-temperature endothermic behavior (T_1) during room-temperature annealing was a result of the destruction of the ordered hard-segment regions. The melt-quenched NH-SiPU2 samples were annealed at 25°C for extended periods to compare the results with the proposed enthalpy relaxation behavior of the hard segment. Figures 8 and 9 indicate that the position and enthalpy of the endothermic peak increased linearly with the logarithm of the annealing time. These find-

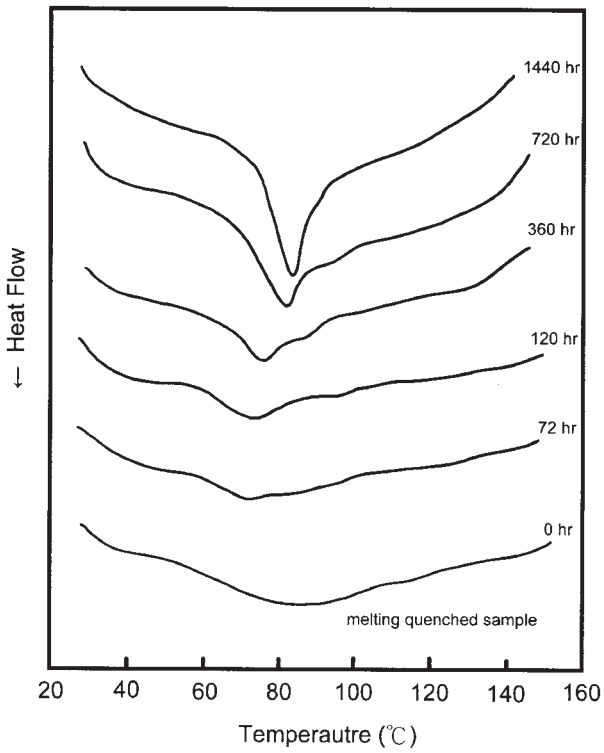

Figure 8 Enthalpy relaxation behaviors of the melt-quenched NH-SiPU2 samples, which were further annealed for different periods of time at 30°C.

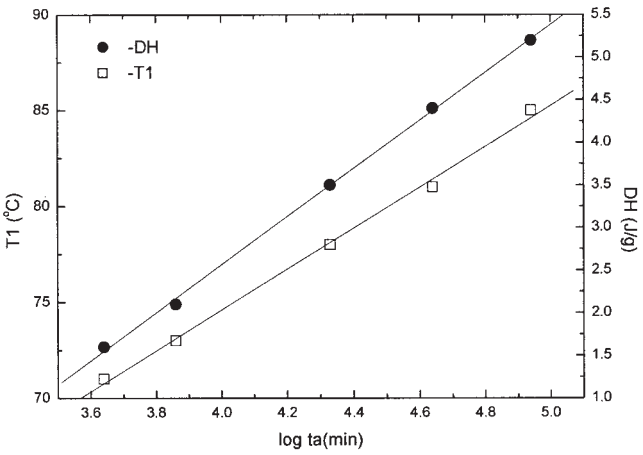

Figure 9 (a) Relationship of the enthalpy, ΔH, and (b) Relationship of endothermic peak position T_1, with respect to the logarithm of the annealing time, t_a. Both (a) and (b) result from the DSC thermograms in Figure 8.

ings verify that T_1 endothermic behavior is probably enthalpy relaxation, resulting from prolonged physical aging form the short-range ordering of the siloxane-hard segment domains (Region I).

Endothermic behavior and morphology of Region II

Figure 5 shows that the reordering or reforming endotherm was terminated at around 150°C and that the endotherm of Region II was not further improved by annealing at 60°C. This result may follow from the fact that the hard-segment domains (Region II) are not disrupted under the annealing conditions, and so the ordered hard-segment domains cannot be further reformed in Region II. However, when the melt-quenched NH-SiPU2 was annealed at 150°C, an ordered structure may be formed again.

Figure 10 displays the DSC thermograms of the melt-quenched NH-SiPU2 samples after annealing at 150°C for different periods. Three endothermic regions, which are associated with the dissociation of the noncrystalline ordered hard segment domains (Region II) [13,16,18,19,29], appeared between 160 and 200°C. Multiple peaks have been frequently observed after annealing at high temperatures.[13,29,31] The first peak (a small shoulder) appeared at about 170°C, just 20°C above the annealing temperature, probably, as stated earlier, because of the enthalpy relaxation of the siloxane hard-segment caused by physical ageing. In fact, the enthalpy relaxation is an enthalpy change that is caused by a change from a nonequilibrium glass state to an equilibrium glass state. Another two endothermic peaks (a small shoulder and the maximum endothermic peak) appeared at around 30°C above the annealing temperature. Hesketh et al. and Seymour and Cooper[13,16] studied the effect of high-temperature annealing on the thermal behavior of PU. Their results are compared with those obtained herein. Endothermic behavior (in the first and second endothermic regions) at high-temperature was caused by the reassociation of mobile siloxane hard-segments and disordered siloxane hard-segments that had moved into more stable and ordered siloxane hard segments. That is, higher-temperature annealing disrupts the long-range ordering of the siloxane hard-segment regions, which are aggregated again and reformed into siloxane hard-segment domains with highly long-range order. Finally, the domains are dissociated at ~30°C above the annealing temperature. Therefore, annealing increased the enthalpy of the endothermic peaks, to an extent that increased with annealing time, as shown in Figure 10. The results showed that high-temperature annealing increased the size and order of the domains. Nearly, all of the peaks were at around the same temperature, suggesting that the positions of the higher-temperature endotherm were independent of the annealing time. The results also demonstrate that a stabilized domain structure was formed under this annealing condition.

Movable siloxane hard segment

Figures 9 and 10 indicate that T_1 was completely absent when the annealing temperature exceeded 150°C. Cooper et al.[13,16] investigated PUs and noted that high-temperature annealing eliminated the T_1. Such annealing increased the temperature of the endothermic peak (T_1), until it merged with T_2, and so eventually only a single endothermic peak was present. The results reveal that the Region I structure was more

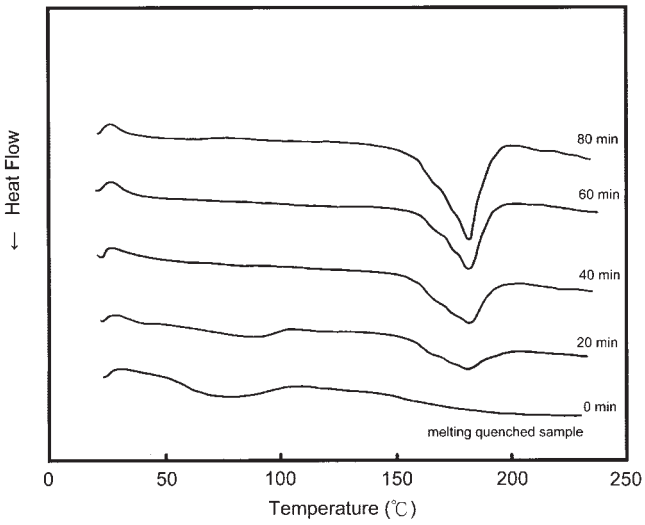

Figure 10 DSC thermograms of the melt-quenched NH-SiPU2 samples, which were annealed at 150°C for different periods.

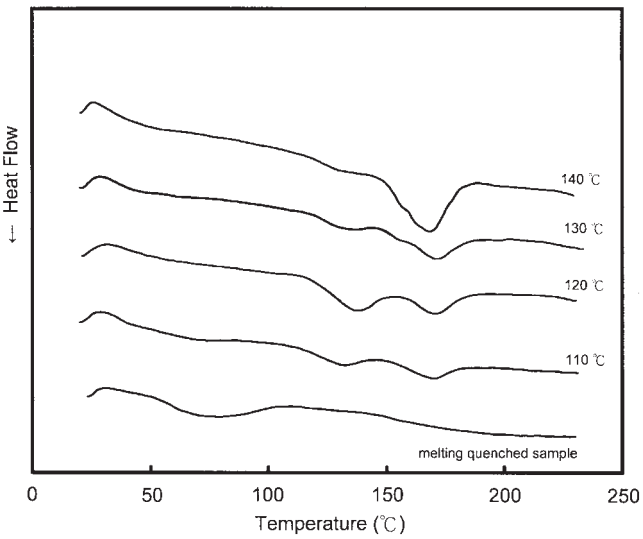

Figure 11 DSC thermograms of the melt-quenched NH-SiPU2 samples, which were further annealed under different annealing temperatures, T_a, for 1 h.

easily moved as the annealing temperature increased, and can merge with the Region II structure. Additionally, annealing can move the T_1 peak (Region I), without creating a well-developed T_2 peak (Region II).

The motion of Region I and the morphology changes; therefore, the melt-quenched NH-SiPU2 samples were annealed at moderate temperatures between 110 and 140°C for 1 h, as plotted in Figure 11, for investigating the movable ability of the siloxane hard-segment domain (Region I). Figure 11 reveals that a small endothermic peak was present at about 20°C above the annealing temperatures (110, 120, and 130°C). The result is consistent with the relationship $T_1 - T_a \approx 20$°C. However, the small endothermic peak almost disappeared after annealing at 140°C, and merged into the endothermic range of Region II. Furthermore, the positions and sizes (T_2 peak) at annealing temperatures between 110 and 130°C remained almost constant. However, the T_2 size clearly increased when the annealing temperature increased to 140°C, because the temperature of the T_1 peak (Range I) entered the T_2 range and combined with T_2 (Range II). The results demonstrate that Range II for NH-SiPU2 develops poorly below the annealing temperature of 140°C.

The melt-quenched NH-SiPU2 samples were annealed at 120°C for different periods, as displayed in Figure 12, to demonstrate further the T_1 behavior associated with enthalpy relaxation at moderate temperatures. Figure 12 indicates that the position and enthalpy of the T_1 peak increased with the annealing time. Figure 13 plots the linear relationships between both the temperature position and the enthalpy of the T_1 peak with the logarithm of the annealing time (log t_a). Figures 12 and 13 demonstrate that the behavior of T_1 is that of enthalpy relaxation, caused by physical aging of the amorphous NH-SiPU2 polymer.

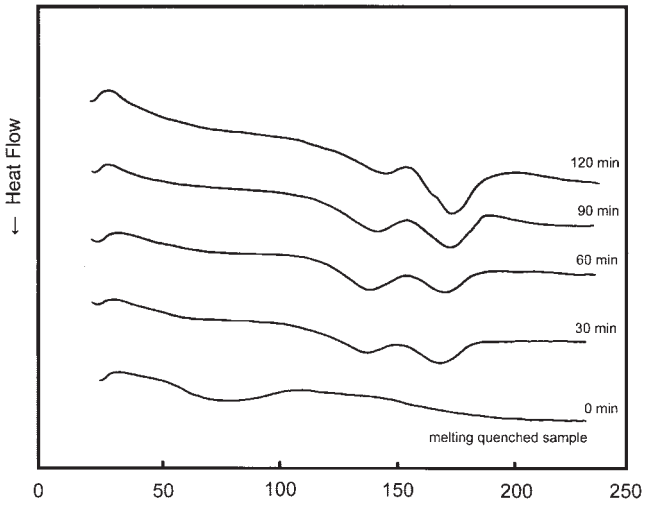

Figure 12 DSC thermograms of the melt-quenched NH-SiPU2 samples, which were annealed at 120°C for different periods.

Waxd analysis

Figure 14 presents the WAXD scan of the melt-quenched NH-SiPU2 sample annealed at 150°C for 1 h. The WAXD intensity and pattern exhibited a completely amorphous structure, revealing that the endothermic behavior following annealing did not involve melting crystallization. This result demonstrated that Regions I and II consisted of amorphous siloxane hard segments.

Morphology of Regions I and II

As stated in the preceding section, DSC elucidated the endothermic behaviors of siloxane hard-segment domains and the relationship between the morphologies

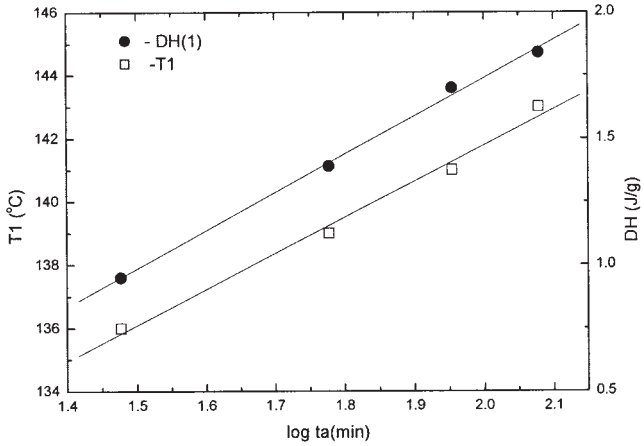

Figure 13 (a) Relationship of the enthalpy, ΔH, and (b) Relationship of endothermic peak position T_1, with respect to the logarithm of the annealing time, t_a. Both (a) and (b) result from the DSC thermograms in Figure 12.

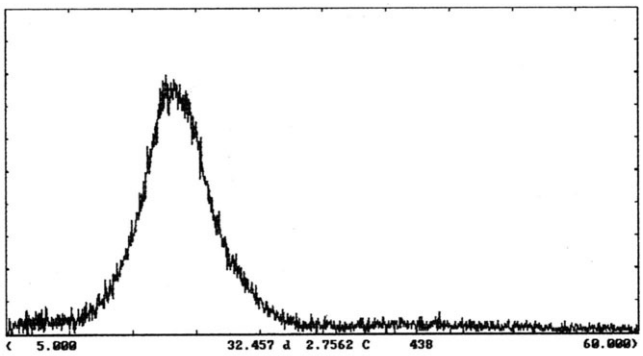

(a)NH-SiPU2

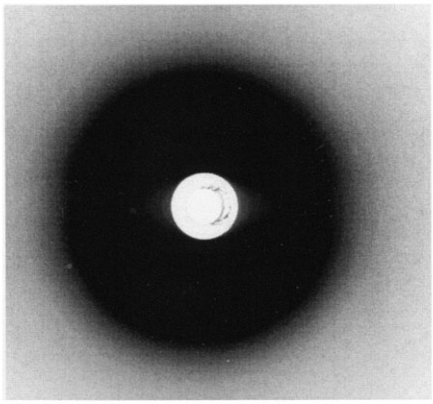

(b)NH-SiPU2

Figure 14 WAXD intensity and pattern of the melt-quenched sample NH-SiPU2 at 140°C annealing for 1 h.

and the domains of the hard-segment. Moreover, better annealing conditions yielded more complete structures of the domain (Regions I and II). Despite the fact that DSC analyzed the morphologies and endothermic behaviors of the siloxane hard-segment domains herein, no definite morphologies of the siloxane hard-segment domains under suitable annealing conditions were obtained. Figures 15 and 16 present the TEM patterns of the melt-quenched NH-SiPU2 samples annealed at 80 and 140°C for 1 h, to elucidate the morphological features of siloxane hard-segment domains (Regions I and II). The TEM image shows that the silioxane hard-segment domains clearly include metallic elements, which are indicated by the white arrow in Figure 15. Furthermore, the amount and distribution of siloxane hard-segments in the domain can be easily estimated from the pattern and the formation of Regions I and II, because the metallic elements appear on the domains. Figure 15 reveals that the hard segment domain (Region I) with short-range order, which contained at least seven siloxane hard-segment groups, was almost circular, with a diameter of 200–500 nm. The siloxane groups are arranged on the edges of the domains, favoring the creation of optical materials. Two small domains, which were formed by the aggregation of urethane hard segments, caused by the intermolecular hydrogen bonds in the segment, were present in the upper right of the pattern. Figure 16 displays the long-range ordering of the hard segment domain (Region II), and the two small Regions I gradually merged with Region II to form a domain with a size of ~800 nm (indicated by a dashed arrow; the white arrow indicates the siloxane groups).

CONCLUSIONS

Siloxane-containing segmented PU consists of two-phase structures include hard and soft-segment phases. Therefore, the DSC thermogram potentially exhibited four phase transition temperatures, although usually fewer than four phase transition temperatures are observed because of the compositions of the soft and hard segments, the extent of phase-separation, and the thermal history.

In this work, the DSC and WAXD analysis of the melt-quenched NH-SiPU2 sample revealed a high degree of phase-separation and amorphous siloxane hard-segment domains, elucidating the endothermic behaviors and morphology of the amorphous siloxane hard-segment domains. The domains comprised silox-

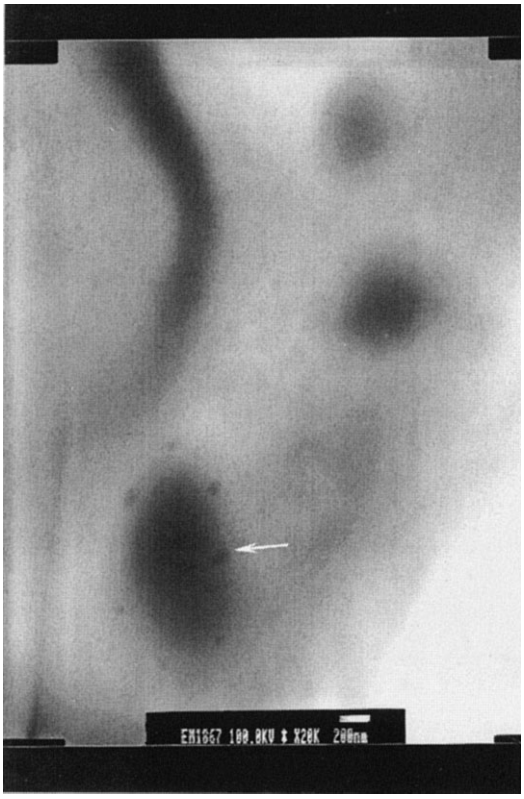

Figure 15 TEM pattern of the melt-quenched NH-SiPU2 sample, which was annealed at 80°C for 1 h.

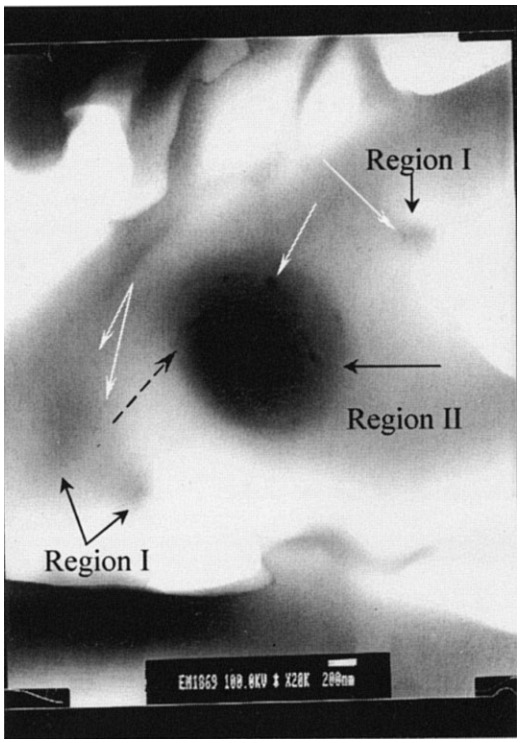

Figure 16 TEM pattern of the melt-quenched NH-SiPU2 sample, which was annealed at 140°C for 1 h.

ane hard segments, which form ordered hard-segment regions (Regions I and II), during extensive annealing. The endothermic nature of T_1 in Region I was associated with enthalpy relaxation behavior caused by prolonged physical aging. The endothermic nature of T_2 in the highly stable Region II exhibited the enthalpy relaxation behavior of the siloxane hard segments with long-range ordering, and the reformation and dissociation of the amorphous siloxane hard-segment domains with long-range ordering. The morphologies of Regions I and II were observed) by TEM, which established that the structures were almost circular, and aggregated by ordered amorphous siloxane hard segments. The DSC thermograms and TEM photograph verified that the moveable structure of Region I was able to merge with the stable structure of Region II, when the annealing temperature exceeded 140°C. The stable Region II structure was formed at a suitable annealing temperature, and so the long-range siloxane hard-segment domains improved the mechanical properties of the PU materials. These domains acted as filler particles for the rubbery soft-segment matrix. The formation of the stable structure in Region II facilitates the manufacture of elastic fibers and elastic fabric, because spinning, dyeing, and finishing usually occur at high temperature.

References

1. Masiulanis, B.; Zielinski, R. J Appl Polym Sci 1985, 30, 2731.
2. Lin, M.-F.; Shu, Y.-C.; Tsen, W.-C.; Chuang, F.-S. Polym Int 1999, 48, 433.
3. Petrovic, S.; Zavargo, Z.; Flynn, J. H.; Mackinght, W. J. J Appl Polym Sci 1994, 51, 1087.
4. Lin, M.-F.; Tsen, W.-C.; Shu, Y.-C.; Chuang, F.-S. J Appl Polym Sci 2001, 79, 881.
5. Chuang, F.-S.; Tsen, W.-C.; Shu, Y.-C. Polym Degrad Stab 2004, 84, 66.
6. Lin, M.-F.; Wang, H. H.; Chuang, F.-S.; Shu, Y.-C.; Tsen, W.-C. J Polym Res 1996, 3, 105.
7. Ferguson, J.; Petrovic, Z. Eur Polym Mater 1973, 12, 177.
8. Gassie, N.; Zulfiqar, M. J Polym Sci Polym Chem Ed 1978, 16, 1563.
9. Grassie, N. Polym Eng Sci 1982, 22, 1057.
10. Ballistreri, S.; Foti, P.; Maravigva, G.; Scamporrino, E. J Polym Sci Polym Chem Ed 1980, 18, 1923.
11. Gaboriaud, F.; Vantelon, J. P. J Polym Sci Polym Chem Ed 1982, 20, 2063.
12. Petrovic, Z. S.; Budinski-Simedic, J. Rubber Chem Technol 1985, 58, 685.
13. Hesketh, T. R.; Van Bogart, J. W. C.; Cooper, S. L. Polym Eng Sci 1980, 20, 190.
14. Clough, S. B.; Schneider, N. S. J. Macromol Sci Phys 1968, 2, 553.
15. Miller, G. W.; Saunders, J. H. J Polym Sci Part A-1: Polym Chem 1968, 8, 1923.
16. Seymour, R. W.; Cooper, S. L. Macromolecules 1973, 6, 48.
17. Seymour, R. W.; Cooper, S. L. J Polym Sci Part B: Polym Lett 1971, 9, 689.
18. Leung, L. M.; Koberstein, J. T. Macromolecules 1986, 19, 707.
19. Koberstein, J. T.; Russell, T. P. Macromolecules 1986, 19, 714.
20. Seymour, R. W.; Estes, G. M.; Cooper, S. L. Macromolecules 1970, 3, 579.
21. Fridman, I. D.; Thomas, E. L. Polymer 1980, 21, 388.
22. Xu, M.; MacKnight, W. J.; Chen-Tsai, C. H. Y.; Thomas, E. L. Polymer 1987, 28, 2183.
23. Foks, J.; Michler, G.; Nanman, I. Polymer 1987, 28, 2195.
24. Richardson, M. J.; Savill, N. G. Polymer 1977, 18, 413.
25. Ellis, T. S. Macromolecules 1990, 23, 1494.
26. Shu, Y. C.; Lin, M. F.; Tsen, W. C.; Chuang, F. S. J Appl Polym Sci 2001, 81, 3489.
27. Lin, M. F.; Shu, Y. C.; Tsen, W. C.; Chuang, F. S. J Appl Polym Sci 2001, 81, 3502.
28. Wang, G.; Fang, B.; Zhang, Z. Polymer 1994, 35, 3178.
29. Van Bogart, J. W. C.; Bluemke, D. A.; Cooper, S. L. Polymer 1981, 22, 1428.
30. Van Bogart, J. W. C.; Gibson, P. E.; Cooper, S. L. J Polym Sci Polym Phys Ed 1983, 21, 65.
31. Chen, T. C.; Shieh, T. S.; Chi, J. Y. Macromolecules 1998, 31, 1312.
32. Tenbrinke, G.; Grooten, R. Colloid Polym Sci 1989, 267, 992.
33. Agrawal, A. J Polym Sci Part B: Polym Phys 1989, 27, 1449.
34. Hodge, I. M.; Berens, A. R. Macromolecules 1982, 15, 767.
35. Shen, J.; Shao, Z.; Li, S. Polymer 1995, 36, 3479.
36. Hourston, D. J.; Song, M.; Hammiche, A.; Pollock, H. M.; Reading, M. Polymer 1996, 37, 243.
37. Bosma, M.; Tenbrinke, G.; Ellis, T. S. Macromolecules 1988, 21, 1465.
38. Mc Gowan, C. B.; Kim, D. Y.; Blumstein, R. B. Macromolecules 1992, 25, 4568.
39. Hodge, I. M. Macromolecules 1983, 16, 899.